The SNEG-13 neutron source: characteristics of the neutron and γ-ray fields

Vit. D. Koval'chuk and A. V. Krasil'nikov

Troitsk Institute of Innovative and Thermonuclear Research, 142092, Troitsk, Moscow Oblast

V. M. Bagaev, S. I. Bobrovnik, Vas. D. Koval'chuk, V. I. Trotsik, and Yu. P. Martakov

Atombezopasnost' Center

V. S. Troshin

Moscow Engineering-Physics Institute

G. G. Voronin, M. P. Svin'in, and A. I. Solnyshkov

D. V. Efremov Scientific-Research Institute of Electrophysical Apparatus, St. Petersburg

D. V. Orlinskiĭ

Kurchatov Institute Russian Science Center, Moscow

(Submitted 18 November 1992; resubmitted 5 May 1993)
Zh. Eksp. Teor. Fiz. **104**, 2577–2589 (August 1993)

The basic characteristics of the SNEG-13 neutron source, with a DT-neutron yield of 10^{13} n/s, are reported. Theoretical estimates of the neutron spectrum are reported. Measurements of the characteristics of the neutron and γ-ray fields behind the target of the neutron source are reported. The γ-ray component of the total dose of ionizing radiation is less than 5%. The scattered-neutron component is 1%. The shape of the DT-neutron line has been studied. The spectrum of the neutron radiation reconstructed from the readings of activation detectors and a silicon semiconductor detector is reported. The capabilities of this neutron source for use in research on the radiation resistance of various systems of the ITER international tokamak fusion reactor are described.

Research on controlled thermonuclear fusion is one of the highest-priority efforts in nuclear power today. The work being carried out by the international community in this field has as its most immediate goal the development by 2005 of the ITER experimental device,[1] which is to serve as a prototype for fusion reactors of the future.

Reaching this goal will require carrying out a broad range of research in various fields of modern physics: plasma physics, nuclear physics, materials science, instrumentation, etc. The success of this research depends in turn on specialized, largely unique experimental apparatus.

Solving the fairly long list of applied problems involved here requires experimental installations which can simulate the radiation conditions which will prevail in the fusion reactor to be developed. Among these problems are problems in radiation materials science and the experimental development and calibration of certain diagnostic systems (e.g., systems for neutron diagnostics). The conditions in the corresponding experiments must come as close as possible to the actual fusion reactor conditions under which the various elements or systems will be used.

The only currently acceptable way to carry out such research is to obtain radiation from intense neutron sources, such as RTNS-II (US), FNS, OCTAVIAN (Japan), and SNEG-13 (Russia).[2]

Planning and executing specific experiments require information on not only the intensity characteristics of these installations but also the detailed structure of the radiation fields created in the volume in which the samples are to be irradiated. These characteristics have been studied for the SNEG-13 neutron source and are being reported here.

1. GENERAL CHARACTERISTICS OF THE FACILITY

The SNEG-13, a special neutron source, was developed and constructed at the Scientific-Research Institute of Electrophysical Apparatus in St. Petersburg as a high-intensity source of neutrons, which are produced in thermonuclear fusion reactions (DD and DT reactions). This source is intended for solving a variety of problems in applied nuclear physics.

The source operates on the basis of the interaction between a beam of deuterium nuclei accelerated to a specified energy and tritium nuclei (in the case of DT reaction) or deuterium nuclei (DD). The latter tritium or deuterium nuclei are absorbed in a titanium layer on a disk-shaped copper target. As the source operates, the deuteron beam is scanned in a circle over the working region (the zone containing the deuterium or tritium) on the fixed target. The zone in which the neutrons are produced is a disk with a thickness which is determined by the range of the deuterons in titanium hydride and which depends on the energy of the deuterons (at a deuteron energy of 300 keV the range is 2.5 μm). This disk has a diameter of 10–40 cm, which can be varied by varying the magnetic field of the deflecting system. Its thickness is about 1 cm and depends on how tightly the beam is focused. The region in which test samples can be placed is 6 mm away from the neutron

 1063-7761/93/080169-07$10.00

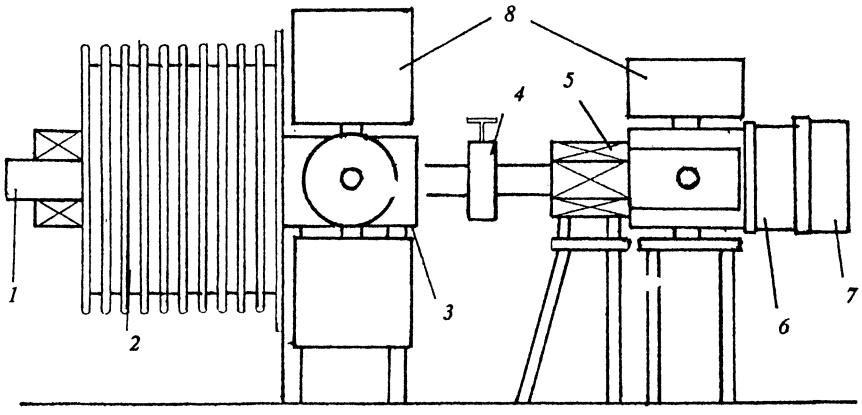

FIG. 1. Layout of the basic parts of the neutron source. *1*—Deuteron source; *2*—accelerating tube; *3*—vacuum chamber; *4*—gate; *5*—system for scanning the beam over the target; *6*—scanning chamber; *7*—target assembly; *8*—roughing pumps.

production zone. This distance is determined by the thickness of the structural elements of the target assembly (2 mm of copper, 2 mm of water, and 2 mm of steel). The water is used as a coolant to relieve the heat load on the source target.

Figure 1 shows the overall arrangement of the various parts of the apparatus. The source is in an experiment hall 12.0 m high. The basic technical specifications of the device are given in Table I. The integral characteristics of the radiation fields of the apparatus are given in Table II.

Whether the DT or DD reaction is used is determined by the type of target. The DT regime is the basic one, and it is for this regime that the measurements reported here were carried out.

2. CHARACTERISTICS OF THE NEUTRON FIELDS OF THE SOURCE

The neutron field in the irradiation zone is shaped by several physical processes and by the structural features of the source. In the first place, the neutrons produced in the DT reaction are not strictly monochromatic: Their energy depends on the deuteron energy and on the angle at which the neutrons are emitted with respect to the direction in which the deuterons are moving. These circumstances ultimately determine the lineshape, which depends on the operating conditions of the source and on the coordinates of the measurement point. In addition, the scanning of the deuteron beam over the target and thus the periodic variation in the distance from the target region emitting the neutrons at the given instant to the sample being irradiated cause cyclic variations in the intensity of the neutron field. Finally, the neutron field contains not only neutrons produced directly in DT reactions but also neutrons scattered in structural elements and the surroundings of the source.

TABLE I. Basic technical specifications of the SNEG-13 neutron source.

Deuteron current	10–100 mA
Deuteron energy	100–300 keV
Target diameter (overall)	43 cm
Diameter of tritium layer	15–40 cm
Width of deuteron beam at target surface	1.5–2.5 cm
Frequency at which the deuterons are scanned over the target surface	50 Hz
Tritium activity in working layer	above 2.5 kCi
Operation	continuous

2.1. Analytic and numerical methods for determining the unscattered neutron radiation

We begin with the time evolution $I(t)$ of the neutron intensity at the point with coordinates x,y,z (the origin is at the center of the target, and z is the distance from the target) due to the circular scanning, with a radius R, of the deuteron beam over the target. We assume that the emitting volume is a point source at each instant. We assume that the cross section for the DT reaction is spatially isotropic in the laboratory frame of reference. We ignore tritium burning in the titanium active layer of the target; this is a legitimate simplification for the actual operating regimes of this source. The time evolution of the intensity is then given by

$$I(t)=\frac{C}{[x-R\cos(2\pi wt)]^2[y-R\sin(2\pi wt)]^2+z^2}, \tag{1}$$

where C is a normalization constant which depends on the neutron yield at the given instant ($C=P/4\pi$, where $P=10^{13}$ n/s at the initial time), R is the radius at which the deuteron beam is scanned over the target surface, w is the scanning frequency (50 Hz), and z is the distance from the titanium surface of the target. Structural features of the

TABLE II. Characteristics of the radiation fields of the SNEG-13 neutron source.

Energy of DT neutrons	14.6 MeV
Neutron yield	$1.0\cdot10^{13}$ n/s (DT) $4.5\cdot10^{10}$ n/s (DD)
Neutron flux density	
behind target surface	$3\cdot10^{11}$ n/(s·cm^2) (DT)
at the sample position	$1.5\cdot10^{8}$ n/(s·cm^2) (DD)
Fluence over run	$5\cdot10^{13}$ n/cm^2 (DT)
γ-Ray dose behind the target (as a percentage of the neutron dose)	5%
Fluence of scattered neutrons (as a percentage of the fluence of fusion neutrons)	1%

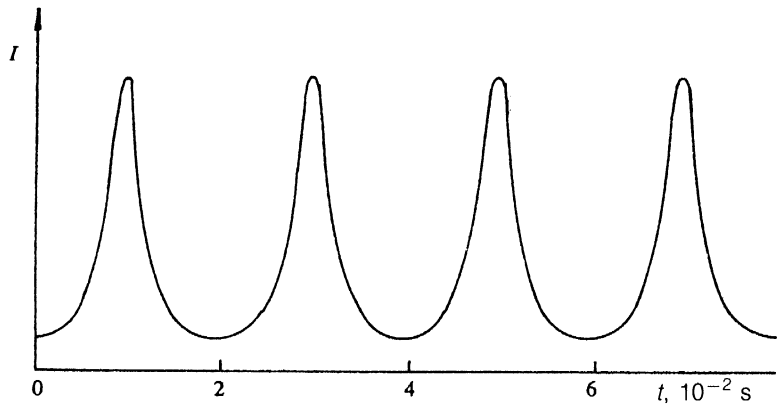

FIG. 2. Time evolution of the neutron radiation for a point on the target surface at the scanning radius.

target of the neutron source impose a lower limit of 6 mm on z (2 mm of copper+2 mm of water+2 mm of steel).

Figure 2 shows the time evolution of the neutron intensity for points on the target surface ($z=0.6$ cm) opposite the working layer ($x^2+y^2=R^2$, where $R=20$ cm, and $Q=10^{13}$ n/s). The samples being bombarded are subjected to an approximately pulsed effect in this case. The ratio of the maximum and minimum amplitudes is 10^3. If the bombardment point is moved toward the center of the target or moved away from the surface of the target, to a distance greater than three times the scanning radius, the irradiation becomes approximately static.

Changes in the coordinates of the bombardment point lead to changes in the time-average flux loads on the test sample (although small in comparison with those for the case of a point source, in which, for example, the deuteron beam is fixed and the target is rotated). This situation is illustrated by Fig. 3, which shows fluence contour levels ($F=3\cdot 10^8$, 10^9, $3\cdot 10^9$, and 10^{10} n/cm^2) beyond the target surface in the plane passing through the center of the target along the x and z axes (for a total neutron yield $P=10^{13}$ n/s and an exposure time of 1 s). These curves are described analytically by the following expression under the approximations adopted above:

$$F(x,z)=\frac{P/4\pi}{[(z^2+x^2+R^2)^2-4\pi R^2x^2]^{0.5}}\cdot \qquad (2)$$

All the results reported above ignore the attenuation of the neutron radiation by structural elements of the source target. This simplification is completely justified since these elements are thin (6 mm). Further evidence for the validity of this simplification comes from the fairly good agreement between the results found here and the experimental results of Ref. 3. The only point which must be kept in mind is that if the source is operated for a long time (tens of hours or more) the tritium in the target may be burned up in a nonuniform way over the circle. If this happens, the distributions found above will change.

For a detection point with a radius vector $\mathbf{r}$, the spectrum of neutrons produced in the DT reaction is

$$f(E_n,\mathbf{r})=\frac{1}{4\pi}\int_V \frac{d\mathbf{r}}{(\mathbf{r}-\mathbf{r}_0)^2}\sigma(E_d(\mathbf{r}_0))\rho(\mathbf{r}_0)$$
$$\times S\left(E_d,E_n\frac{\mathbf{r}(\mathbf{r}-\mathbf{r}_0)}{|\mathbf{r}||\mathbf{r}-\mathbf{r}_0|}\right), \qquad (3)$$

where E_d is the energy of the deuterons at point $\mathbf{r}$ (this energy varies as a result of the stopping of the deuterium in the substrate material), ρ is the tritium concentration in the target, σ is the energy dependence of the cross section for the DT reaction, $\mathbf{r}_0$ is the vector along the direction of the accelerated deuterons, S is the angular distribution of

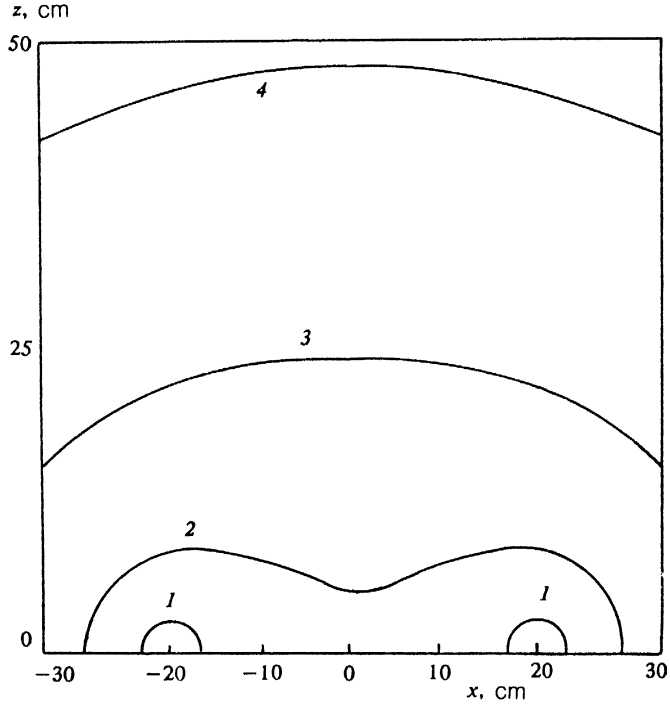

FIG. 3. Contour curves for fluences $F=10^{10}$, $3\cdot 10^9$, 10^9, and $3\cdot 10^8$ n/cm^2 (curves *1–4*, respectively) in the plane perpendicular to the target surface and passing through the center of the target. The total neutron yield is 10^{13} n/s; the scanning radius is 20 cm.

the spectrum of DT neutrons, and V is the volume in which the DT reaction occurs for the given working conditions of the apparatus.

In the approximation $\rho=\text{const}$, $dE/dx=\text{const}$, expression (3) simplifies:

$$f(E_n,R)=\int \frac{\sigma(E_d)(E_n+a\chi E_d)E_d}{R^2 b^{0.5}(E_n-a\eta E_d)^9}\,dE_d, \qquad (4)$$

where

$$a=\frac{m_d m_n}{(m_d+m_n)^2},\quad \chi=\frac{m_d+m_{\mathrm{He}}}{m_d m_n}\left(m_{\mathrm{He}}-m_t+\frac{m_{\mathrm{He}}Q}{E_d}\right),$$

$$b=1-\frac{R^2-R_0^2}{2RR_0}-\frac{H^2}{2RR_0}\left(\frac{4aE_dE_n}{(E_n-a\chi E_d)^2}-1\right)^2.$$

Here m_d, m_n, m_{He}, and m_t are the masses of the interacting particles and reaction products; R is the radius of the scanning of the deuteron beam over the target surface; R_0 is the distance from the center of the scanning ring to the detection point; H is the distance from the detection point to the target surface; and Q is the energy of the fusion reaction.

It follows from the general form of expression (3) that the shape of the spectrum is determined by parameters associated with the working conditions of the apparatus: the energy of the accelerated deuterons and the profile of the tritium concentration in the working layer of the target. This profile may vary during operation of the source, because of tritium diffusion into the evacuated volume and a replacement of the tritium by deuterium nuclei.

Figure 4 shows spectra found for certain points behind the target source which are of practical interest, for various values of E and of the functions $\rho(\mathbf{r}_0)$, through numerical integration of Eqs. (3) and (4). These results were obtained with the help of σ and S values from Ref. 4 and ρ and dE/dx values from Ref. 5.

2.2. Experimental differential characteristics of the neutron fields

The spectrum of the neutron emission was studied experimentally with activation and silicon semiconductor detectors.

In the case of the semiconductor detectors, the procedure[6] involves detecting products of the reactions $^{28}\mathrm{Si}(n,p)^{28}\mathrm{Al}$ and $^{28}\mathrm{Si}(n,\alpha)^{25}\mathrm{Mg}$, which neutrons cause directly in the detector material. Because of the good energy resolution of the semiconductor detectors (1–2%) and the unambiguous relationship between the energy of the reaction products and the energy of the neutrons inducing the reactions, we can determine the shape of the neutron spectrum from the instrumental lineshape.

A surface-barrier silicon detector with a working layer 1.5 mm thick was used. Figure 5 shows instrumental spectra measured at a deuteron acceleration voltage of 150 keV for various spatial points.

These spectra were analyzed by means of algorithms which employ regularization methods for solving the Fredholm equation.[6] Data from Refs. 8 and 9 on the characteristics of the nuclear reactions $^{28}\mathrm{Si}(n,p)^{28}\mathrm{Al}$ and $^{28}\mathrm{Si}(n,\alpha)^{25}\mathrm{Mg}$ are used in these calculations.

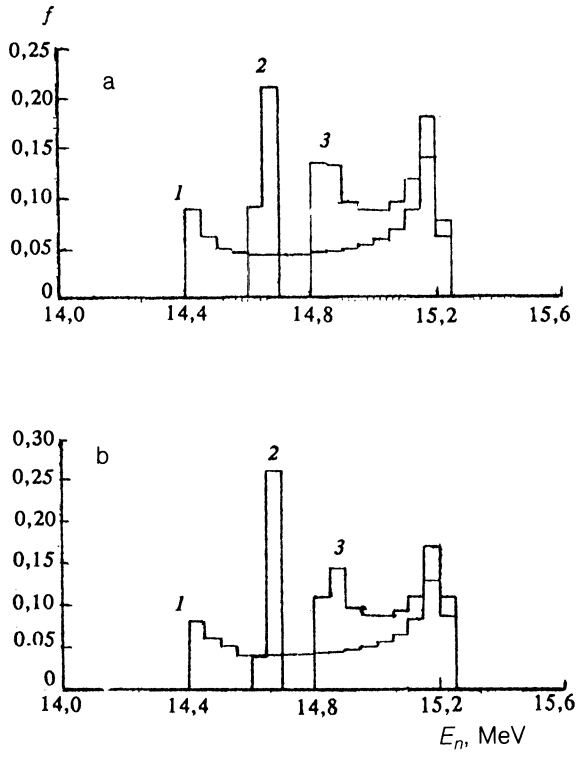

FIG. 4. Calculated neutron spectrum of the source. a—For a function $r(\mathbf{r})=\text{const}$; b—$\rho(\mathbf{r})=10$. Histogram *1*) Spatial points with the coordinates ($x=0$, $y=0$, $z=10$ cm); *2*) ($x=10$ cm, $y=0$, $z=30$ cm); *3*) ($x=10$ cm; $y=0$, $z=10$ cm). The origin is at the center of the target.

Qualitative information on the variations in the neutron spectrum from the SNEG-13 as a function of the spatial coordinates of the detection point can also be found from experiments based on activation integrals of detectors which differ in the energy dependence of the reaction cross sections in the energy range of the DT neutrons. We used detectors based on the reactions $^{19}\mathrm{F}(n,2n)$ and $^{27}\mathrm{Al}(n,\alpha)$. The ratios of the activation integrals of these reactions were found as functions of the energy of the monoenergetic neutrons near 14 MeV in experiments on the NGM-150 neutron source (a special standard) at the VNIIFTRI Research and Production Association.

In studies of the characteristics of the radiation, these pairs of detectors were placed at various points behind the source target. Effective neutron energies were found from measurements of the ratios of activation integrals. The results are shown in Table III.

Characteristics of the neutron radiation over the entire range (from thermal energies up to 20 MeV) were studied with the help of a special set of activation detectors. To determine the general aspects of the formation of the scattered-radiation fields, measurements were carried out not only in the spatial regions of practical interest for irradiation experiments but also at a significant distance from the source target. The qualitative behavior found is reported below, along with some quantitative results on the

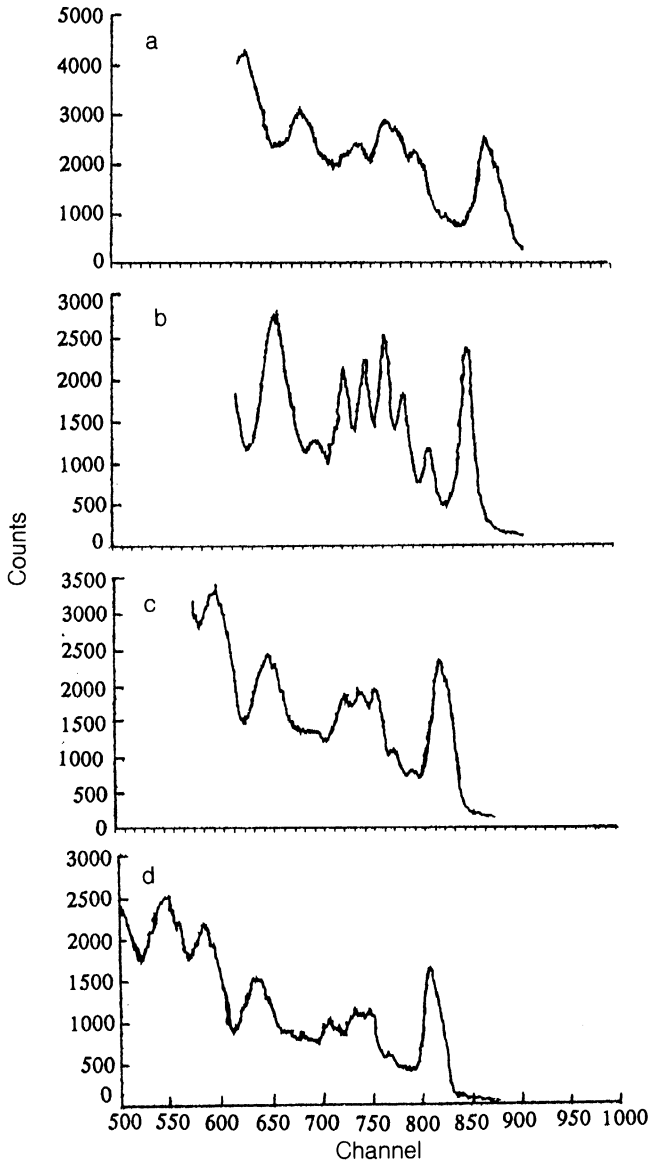

FIG. 5. Instrumental spectra of a silicon detector for various spatial points. a—($x=0$, $y=0$, $z=300$ cm); b—($x=30$ cm, $y=0$, $z=0$); c—($x=17$ cm, $y=0$, $z=10$ cm); d—($x=150$ cm, $y=0$, $z=0$).

overall spectrum of the neutron radiation (referred to a total neutron yield of $5.4 \cdot 10^{15}$ n from the target).

Thermal neutrons. The measurements were carried out with Au, Na, and Dy detectors. The thermal-neutron fluence was calculated by the "cadmium difference" method. Each detector was irradiated twice: inside a cadmium sheath and without it. The "above-cadmium" fraction of the activity was then subtracted.

From these results we can draw conclusions about the formation of the thermal-neutron field as the result of thermalization of DT neutrons in the walls of the source hall. The thermal-neutron fluence is essentially constant at $5.5 \cdot 10^8$ n/cm^2 at all points in the hall, including the volume behind the target. As the measurement point is moved out of the source hall, the thermal-neutron fluence drops sharply.

Fast neutrons. The field of fast neutrons (0.1 MeV $< E_n <$ 15 MeV) was studied with a larger set of threshold activation detectors. Analysis of the spatial variation of this field led to the conclusion that the scattered radiation consisted of two components: neutrons scattered directly in structural elements of the target assembly (the fluence of the scattered neutrons decreases significantly with distance from the target) and neutrons reflected from the walls of the hall (the variation of the neutron fluence is not in inverse proportion to the square of the distance from the center of the target). A quantitative estimate of the spectral characteristics was found from measurements using the complete set of activation detectors at a point 10 cm away from the working layer of the target; this point corresponds to the typical position of the test samples in the irradiation experiments. Experimental data corresponding to this point are shown in Table IV.

The values of the activation integral A_0 are referred to a single nucleus of the isotope:

$$A_0 = \frac{1}{N} \int \sigma(E)\Phi(E)dE, \tag{5}$$

where $\sigma(E)$ is the energy dependence of the activation cross section of the detector, $\Phi(E)$ is the neutron spectrum, and N is the number of nuclei of the isotope in the detector.

The neutron energy spectrum at the detection point was reconstructed from the experimental data with the TDN code (Moscow Engineering-Physics Institute). This code was written especially for reconstructing fusion or source neutron spectra from the readings of activation detectors. Information of the shape of the peak found by the methods described earlier was used in analyzing the spectral shape.

To reconstruct the neutron radiation spectrum we begin by determining the fusion-neutron component and the shape of the peak. The algorithm embodies the information that the peak is Gaussian. For this purpose, we select from the entire set of activation integrals those which correspond to neutron reactions with a threshold near the peak of DT neutrons.

TABLE III. Effective neutron energy at various spatial points on the target surface.

No.	E_{eff}, MeV	Coordinates of point, cm	No.	E_{eff}, MeV	Coordinates of point, cm
1	14,7	20,3; 0	3	14,5	10,8; 14,0
2	14,4	0,8; 10,0	4	14,4	0; 25,0

The coordinate origin is at the lower point of the target.

TABLE IV. Values of the activation integrals.

No.	Nuclear reaction	A_0, 10^{13} s^{-1}	No.	Nuclear reaction	A_0, 10^{13} s^{-1}
1	$^{19}F(n, 2n)$	1,54	8	$^{54}Fe(n, p)$	9,88
2	$^{24}Mg(n, p)$	5,1	9	$^{56}Fe(n, p)$	2,97
3	$^{27}Al(n, p)$	2,0	10	$^{58}Ni(n, p)$	10,1
4	$^{27}Al(n, \alpha)$	3,19	11	$^{58}Ni(n, 2n)$	0,81
5	$^{31}P(n, p)$	2,26	12	$^{46}Ti(n, 2n)$	1,07
6	$^{63}Cu(n, 2n)$	14,8	13	$^{64}Zn(n, p)$	4,77
7	$^{54}Fe(n, 2n)$	0,243	14	$^{103}Rh(n, n^1)$	11,7

From the results of the reconstruction of the DT-neutron spectrum we find the energy $E=14.35$ MeV at the peak of the spectrum. We also find the width of the spectrum at half-maximum, 1.45 MeV. The discrepancy between the experimental and theoretical activation integrals for this specification of the spectrum is less than 0.5% in the peak region.

The neutron spectrum behind the target of the neutron source reconstructed by the TDN program is shown in Fig. 6. Within the errors in the measurements of the activation integrals, we find no scattered-neutron contribution. For the flux of scattered neutrons with energies above 0.1 MeV (minus DT neutrons) we find an upper limit of $9 \cdot 10^9$ n/cm^2.

3. CHARACTERISTICS OF THE γ-RADIATION FIELD

Although the DT reaction does not involve the production of γ rays, the radiation field at the positions of the test samples during irradiation is mixed. The γ rays are produced in processes which accompany the motion of the accelerated particles in the inner volume of the source (including the active layer of the target) and also in the interaction of DT neutrons with surrounding material.

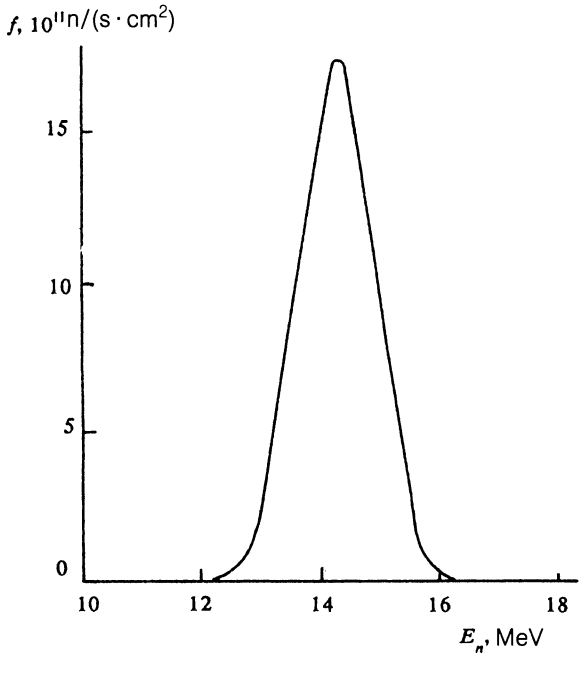

FIG. 6. Neutron radiation spectrum behind the target as reconstructed by the TDN code (Moscow Engineering-Physics Institute).

Characteristics of the γ field and its spectrum were evaluated quantitatively from measurements using ^{6}LiF, ^{7}LiF, $CaSO_4$, and Al_2PO_3 thermoluminescence detectors (the TOLEDO and IKS systems).

Since the effective nuclear charges of the elements in these detectors are different, the detectors differ in the energy dependence of the sensitivity, particularly at low energies. Thus a method like that described in Ref. 10 could be used in analyzing the results. This method uses detectors whose sensitivity is nonzero over the entire energy range of interest. This approach adds to the experimental information on the low-energy part of the spectrum. Characteristics of the bremsstrahlung are reconstructed from the set of results of measurements of the absorbed dose in the thermoluminescence detectors, normalized to the results found during irradiation of the same detectors in a reference field.

In addition, a set of filters to modify the energy dependence of the sensitivity of the detectors was used in the measurements.

A serious problem in analyzing the results of these measurements is the need to deal with the contribution made by neutron radiation to the readings of the thermoluminescence detectors. The data in the literature on this point are rather contradictory, so it was necessary to carry out some additional research. In the course of this research we determined the specific kerma of the neutrons (the spectrum was taken into account) in the detector material, using kerma values from Ref. 10. Using the results of experiments with a californium source, whose field characteristics had been measured with a scintillation detector using a stilbene crystal, we then determined the light yield from the thermoluminescence detectors due to heavy charged particles.

The results found in measurements with the thermoluminescence detectors of all the types used agreed fairly well with each other, after corrections for neutron sensitivity. The γ-radiation dose behind the target of the neutron source (at distances up to 10 cm) amounts to about 5% of the neutron dose. From an analysis of the measurements carried out with various filters and without the filters we can conclude that low-energy γ rays make no significant contribution to the overall dose. The primary source of γ radiation in the near zone of the source (at distances up to

1 m from the target) is the interaction of neutrons with the nuclei of elements making up the structural parts of the acceleration tube and the target assembly of the source (inelastic scattering of fusion neutrons). For these processes, the γ-ray spectrum has an average energy on the order of a few MeV. At large distances from the target the dose is made up primarily of γ rays produced in the walls of the hall.

Yet another characteristic of the γ-ray field of the neutron source is the emission from structural parts activated by neutrons. Measurements show that the γ dose rate behind the target increases by 15–25% after 20–30 min of operation at a constant source power. This increase is evidently due to induced activity. The temporal decay of the activation component after the source is turned off is described by a fairly complicated law, so it is not possible to reliably identify all the partial channels of activation reactions. This characteristic should be taken into account when the source is operated at a low intensity (at a neutron yield less than 10^{12} n/s) right after the completion of work near the nominal intensity.

CONCLUSION

This study of the γ-ray and neutron components of the ionizing radiation field behind the target of the SNEG-13 neutron source leads to the following conclusions.

1. In the volume studied (in the zone in which the samples to be bombarded will presumably be placed), we observe a pure spectrum of fusion neutrons. The contributions of scattered neutrons and γ rays are negligible—less than 5–10% of the dose of fusion neutrons, depending on the particular spatial point. Thus the neutron spectrum expected for a fusion device can be generated by using various composite materials between the surface of the target of the neutron source and the detection point.

2. The shape of the DT neutron peak is complicated and depends on the operating conditions of the source and the state of the target. There are certain source operating conditions under which it is possible to vary the half-width of the energy distribution of fusion neutrons and also their effective energy. This flexibility can be utilized for testing neutron spectrometric systems with a high energy resolution.

3. During prolonged irradiation experiments, the shape of the peak does not affect the results of the irradiation.

4. The gradient of the neutron flux density near the surface of the SNEG-13 target is smaller than in the case of a point source. It thus becomes possible to irradiate objects of finite dimensions more nearly uniformly near the target surface.

5. During steady-state operation of the neutron source, with the test sample at the target surface, the neutron bombardment is approximately pulsed.

6. In the preparation for, and during, irradiation experiments, it is necessary to allow for the neutron spectrum, primarily in monitoring the load fields.

[1] P.-H. Rebut, Preprint, JET Joint Undertaking, Abingdon, Oxon, OX14 3EA, UK, 1992.
[2] Vit. D. Kovalchuk, A. V. Krasilnikov, V. M. Bagaev *et al.*, Preprint IAE-5589/8, Moscow, 1992.
[3] V. M. Bagaev, Yu. P. Martakov, V. D. Sevast'yanov *et al.*, *Abstracts, Fifth All-Union Conference on the Metrology of Neutron Radiation at Reactors and Accelerators*, NPO VINNFTRI, Moscow, 1990, p. 202.
[4] G. A. Borisov, R. D. Vasil'ev, and V. F. Shevchenko, *Kinematic Tables for (d,n) and (p,n) Nuclear Reactions*, Izd. Standartov, Moscow, 1974.
[5] S. Yamaguchi, Y. Oyama, and H. Maekawa, Preprint, JAERI, 1984, p. 84.
[6] T. Elevant, H. W. Wendel, E. B. Nieschmidt, and L. E. Samuelson, Rev. Sci. Instrum. **57**, 1763 (1986).
[7] A. N. Tikhonov, A. V. Goncharskiĭ, V. V. Stepanov, and A. G. Yagola, *Numerical Methods for Solving Ill-Posed Problems*, Nauka, Moscow, 1990, p. 238.
[8] D. W. Mingay, J. P. E. Seleschop, and P. M. Johnson, Nucl. Instrum. Methods **94**, 497 (1971).
[9] L. I. Klochkova and B. S. Kovrygin, At. Energ. **58**, 375 (1985).
[10] K. A. Baĭgarin, V. F. Zinchenko, V. M. Likhopat, and V. V. Timofeev, At. Energ. **70**, 410 (1991).
[11] R. S. Caswell, J. I. Coyne, and M. L. Rendolph, J. Appl. Radiact. Isot. **33**, 1227 (1982).

Translated by D. Parsons